

1
2
3
4
5
6
7
8
9
10
11
12
13
14
15
16
17
18
19
20
21
22
23
24
25
26
27
28
29
30

C:N:P stoichiometry at the Bermuda Atlantic Time-series station in the North Atlantic Ocean

Arvind Singh^{1,2}, Steven E. Baer³, Ulf Riebesell², Adam C. Martiny⁴, M. W. Lomas^{1,3*}

¹Bermuda Institute of Ocean Sciences, St. George's, GE01, Bermuda

²GEOMAR Helmholtz-Zentrum für Ozeanforschung Kiel, 24105 Kiel, Germany

³Bigelow Laboratory for Ocean Sciences, East Boothbay, ME 04544, USA

⁴University of California, Irvine, California 92697, USA.

*E-mail address of the corresponding author: mlomas@bigelow.org (M.W. Lomas)

31 **Abstract**

32 Nitrogen (N) and phosphorus (P) availability, in addition to other macro-and micronutrients,
33 determine the strength of the ocean's carbon (C) uptake, and variation in the N:P ratio of
34 inorganic nutrient pools is key to phytoplankton growth. A similarity between C:N:P ratios in the
35 plankton biomass and deep-water nutrients was observed by Alfred C. Redfield around 80 years
36 ago and suggested that biological processes in the surface ocean controlled deep ocean
37 chemistry. Recent studies have emphasized the role of inorganic N:P ratios in governing
38 biogeochemical processes, particularly the C:N:P ratio in suspended particulate organic matter
39 (POM), with somewhat less attention given to exported POM and dissolved organic matter
40 (DOM). Herein, we extend the discussion on ecosystem C:N:P stoichiometry but also examine
41 temporal variation of stoichiometric relationships. We have analysed elemental stoichiometry in
42 the suspended POM and total (POM + DOM) organic matter (TOM) pools in the upper 100 m,
43 and in the exported POM and sub-euphotic zone (100 - 500 m) inorganic nutrient pools from the
44 monthly data collected at the Bermuda Atlantic Time-series Study (BATS) site located in the
45 western part of the North Atlantic Ocean. C:N and N:P ratios in the TOM were at least twice that
46 in the POM, while C:P ratios were up to five times higher in the TOM compared to that in the
47 POM. Observed C:N ratios in suspended POM were approximately equal to the canonical
48 Redfield Ratio (C:N:P = 106:16:1), while N:P and C:P ratios in the same pool were more than
49 twice the Redfield Ratio. Average N:P ratios in the subsurface inorganic nutrient pool were
50 ~26:1, squarely between the suspended POM ratio and the Redfield Ratio. We have further
51 linked variation in elemental stoichiometry with that of phytoplankton cell abundance observed
52 at the BATS site. Findings from this study suggest that elemental ratios vary with depth in the
53 euphotic zone mainly due to different growth rates of cyanobacterial cells. We have also

54 examined role of the Arctic Oscillation on temporal patterns in C:N:P stoichiometry. This study
55 strengthens our understanding of the variability of elemental stoichiometry in different organic
56 matter pools and should improve biogeochemical models by constraining the range of non-
57 Redfield stoichiometry and the net relative flow of elements between pools.

58

59 Keywords: North Atlantic Ocean, BATS, Biogeochemistry, Phytoplankton, Stoichiometry

60

61

62 **1. Introduction**

63 Nitrogen (N) and phosphorus (P) are critical elements that control primary production in
64 large portions of the surface ocean. Traditionally, N is considered a proximate and P is an
65 ultimate limiting nutrient in surface waters (Tyrrell, 1999), but primary production in the North
66 Atlantic Ocean has been suggested to be P stressed (Wu et al., 2000; Karl et al., 2001; Sañudo-
67 Wilhelmy et al., 2001; Lomas et al., 2010). Alfred C. Redfield first noted the similarity between
68 N:P ratios in surface ocean particulate organic matter (POM) and in deep-water inorganic
69 nutrients; this observation was further extended to include carbon (Redfield, 1934).
70 Oceanographic studies have consistently found mean plankton biomass to adhere to the Redfield
71 Ratio (C:N:P = 106:16:1; Redfield, 1958; Copin-Montegut and Copin-Montegut, 1983; Geider
72 and La Roche, 2002), and since then this ratio has become a fundamental tenet in marine
73 biogeochemistry. Deviations from the canonical ratio have been used to provide insights into
74 phytoplankton physiology (Goldman et al., 1979; Quigg et al., 2003), nutrient limitation of
75 primary production (e.g., Falkowski and Raven, 1997; Moore et al., 2013), efficiency of
76 biological carbon sequestration in the ocean (Sigman and Boyle, 2000) and the input/output
77 balance of the marine N cycle (e.g., Gruber and Sarmiento, 1997). Geochemists use the
78 Redfield conceptual model to determine the state of the marine N cycle using the N* proxy (e.g.,
79 Gruber and Sarmiento, 1997). In the context of this proxy, subsurface nutrient N:P ratios > 16:1
80 suggest net nitrogen gain, while ratios < 16:1 suggest net nitrogen loss (e.g., Gruber and Deutsch,
81 2014). However, this relatively simple point of view has been shown to yield up to four-fold
82 overestimation of N₂ fixation rates when compared to directly measured rates (Mills and Arrigo,
83 2010). In part, this overestimation is due to the production and sedimentation of non-N₂ fixer
84 biomass that can occur at ratios much greater than Redfield, particularly in the subtropical and

85 tropical oceans (Singh et al., 2013; Martiny et al., 2013; Teng et al., 2014). Furthermore, an
86 ocean circulation model has shown that the N:P ratio of biological nutrient removal varies
87 geographically, from 12:1 in the polar ocean to 20:1 in the sub-Antarctic zone, regions where N₂
88 fixation is not thought to be important (Weber and Deutsch, 2010). With a better understanding
89 of N cycle processes, the validity of the Redfield model for nutrient uptake has been questioned
90 (Sañudo-Wilhelmy et al., 2004; Mills and Arrigo, 2010; Zamora et al., 2010).

91 Biologically speaking, a fixed N:P ratio, like the Redfield Ratio, would suggest that
92 nutrients are taken up in that ratio during production of new organic matter (Redfield, 1958;
93 Lenton and Watson, 2000). This conceptual model has been challenged by the fact that the
94 variability in nutrient requirements is related to the functioning and evolution of microbes
95 (Arrigo, 2005). The N:P ratio in phytoplankton need not be in the canonical ratio and can vary
96 widely from coastal upwelling to transitional to oligotrophic regions of the ocean. The observed
97 ratio varies with taxa and growth conditions (Arrigo et al., 1999; Quigg et al., 2003; Klausmeier
98 et al., 2004). For example, it has been shown that non-Redfield nutrient utilization is common
99 during blooms (Arrigo et al., 1999) and in regions dominated by cyanobacteria (Martiny et al.,
100 2013). The N:P ratio of *Synechococcus* and *Prochlorococcus*, small and abundant phytoplankton
101 cells in the open ocean, varies from 13.3 to 33.2 and 15.9 to 24.4, respectively, during
102 exponential growth, while the ratio can be as high as 100 during PO₄³⁻ limited growth (Bertilsson
103 et al., 2003; (Heldal et al., 2003). Another cyanobacteria, the N₂ fixer *Trichodesmium* has an
104 N:P ratio that varies from 42 to 125 (Karl et al., 1992), while in general diatoms have a ratio of
105 ~11:1 (Quigg et al., 2003; Letelier and Karl, 1996; Mahaffey et al., 2005). Excess downward
106 dissolved organic nitrogen (DON) fluxes relative to NO₃⁻ are associated with *Trichodesmium*

107 abundance (Vidal et al., 1999). Thus the relative abundance of different phytoplankton functional
108 groups may lead to coupling of N and P cycles in non-Redfieldian proportions.

109 Considerable effort has been made to understand the variability and controls on the N:P
110 ratio in the dissolved inorganic nutrient pool (e.g., Gruber and Sarmiento, 1997; Pahlow and
111 Riebesell, 2000; Arrigo, 2005). In contrast, analysis of C:N:P ratios in particulate organic matter
112 (POM) and dissolved organic matter (DOM) are more scarce (Karl et al., 2001; Letscher et al.,
113 2013). The C:N:P ratio however, has great relevance in oceanography, as it connects the
114 ‘currency’ of the ocean, i.e., carbon, to some of its controlling variables, N and P. Here, we
115 present a detailed analysis of C:N:P stoichiometry of POM and TOM along with N:P
116 stoichiometry of dissolved inorganic nutrients at the Bermuda Atlantic Time-series Study
117 (BATS) for an eight year period. The observed ratios are correlated with and discussed in the
118 context of co-measured biological parameters such as cell abundances of different phytoplankton
119 groups and chlorophyll *a*. The goal of this study was to quantitatively assess C:N:P ratios in all
120 (POM, TOM and inorganic nutrients) the pools and their deviations from the Redfield Ratio, and
121 relationships to biogeochemical cycling.

122

123 **2. Methods**

124 **2.1 Data Availability**

125 Since 1988, the BATS site, located in the western subtropical North Atlantic Ocean (31°
126 40’N, 64° 10’W), has provided a relatively unique time–series record of nutrient biogeochemical
127 cycles. However, data on total organic C (TOC), total organic N (TON) and total organic P
128 (TOP) and particulate organic C (POC), particulate organic N (PON), and particulate organic P
129 (POP) have only been collected concurrently since 2004. These data were collected from seven

Comment [MWL1]: New subheadings to break the methods into logical units.

130 different depths (5, 10, 20, 40, 60, 80 and 100 m) over the euphotic zone. We obtained these data
131 from the BATS website (bats.bios.edu) and analysed the data record from 2004-2012.

132

133 **2.2 Analytical Methods**

134 Samples for nitrate (NO_3^-) and phosphate (PO_4^{3-}) were gravity filtered (0.8 μm) and
135 frozen (-20°C) in HDPE bottles until analysis (Dore et al., 1996). NO_3^- and PO_4^{3-} were measured
136 using a Technicon autoanalyser with an estimated inaccuracy of $\sim 0.12 \mu\text{mol kg}^{-1}$ and $0.02 \mu\text{mol}$
137 kg^{-1} , respectively (Bates and Hansell, 2004). The Magnesium Induced Co-precipitation
138 (MAGIC) soluble reactive P (SRP) method (Karl and Tein, 1997) was used starting in late 2004
139 to improve both the sensitivity and the accuracy of the inorganic PO_4^{3-} analysis (Lomas et al.,
140 2010). POC and PON samples were filtered on pre-combusted (450°C , 4h) Whatman GF/F
141 filters (nominal pore size $0.7 \mu\text{m}$) and frozen (-20°C) until analysis on a Control Equipment 240-
142 XA or 440-XA elemental analyzer (Steinberg et al., 2001; Lomas et al., 2013). POP was
143 analyzed using the ash-hydrolysis method with oxidation efficiency and standard recovery
144 checks (Lomas et al., 2010). TOC and TON concentrations were determined using high
145 temperature combustion techniques (Carlson et al., 2010). Total P (TP) concentrations were
146 quantified using a high temperature/persulfate oxidation technique and TOP calculated by
147 subtraction of the MAGIC-SRP value (Lomas et al., 2010). Ideally DOM concentrations would
148 have been estimated by subtracting POM from its total organic concentrations, e.g., $[\text{DOC}] =$
149 $[\text{TOC}] - [\text{POC}]$, but we did not have paired TOC (and TON) and POC (and PON) values;
150 corresponding POC (and PON) values were taken at slightly different depths but on the same
151 sampling day. Nevertheless, subtraction would not have had a substantial impact because, on
152 average, POC and PON values in the upper 100 m were $<4\%$ of TOC and TON, respectively

153 (Fig. 1). Both the accuracy and precision of dissolved organic compound concentrations decrease
154 with depth as concentrations of inorganic nutrients increase to dominate the total pools.

155 Chlorophyll *a* pigments were analyzed by HPLC using the method of van Heukelem and
156 Thomas (2001). Samples for flow cytometric enumeration of pico- and nano-plankton were
157 collected on each cruise and analysed as described in Lomas et al. (2013). Export fluxes of POC,
158 PON and POP were estimated using surface-tethered particle interceptor traps deployed at 200 m
159 depth as described in previous publications (Lomas et al., 2010; Steinberg et al., 2001).
160 Elemental masses of material captured in sediment traps, trap collection surface area and
161 deployment length were used to calculate fluxes (see Lomas et al., 2013 for a more detailed
162 methodology on all the described parameters in the method section).

163

164 2.3 Data Processing

165 Our POM and TOM analysis was restricted to the upper 100 m, which also reflects the
166 approximate mean depth of the euphotic zone at BATS (Siegel et al., 2001) and the zone where
167 nutrients are depleted to near analytical detection. All data presented as elemental ratios are in
168 mol/mol units. Mixed layer depth was defined as a 0.125 kg m⁻³ difference in seawater density
169 from the surface (Gardner et al., 1995). While mixed layer depths (MLD) were always deepest
170 during winter, the exact timing of the deepest mixing shifted between years. For example, during
171 2005, the MLD was deepest in March, while it was deepest during February in 2006. Therefore,
172 when presenting data on an annual cycle, we aligned our data to the measured timing of deep
173 mixing in each year and combined all the data to a single 12 month composite (e.g., Carlson et
174 al., 2009). Generally the mixed layer depth was no deeper than ~25m in summer, thus we used

175 this depth range, 0-25m, to represent the 'surface' data and present our analysis in two depth bin,
176 0-25m and 25-100m.

177

178 3. Results

179 We present time-series data of chemical constituents in POM and TOM pools (Fig. 1). We
180 further calculated depth-averaged ratios of the chemical constituents. We first calculated average
181 concentration of each element over the depth segment (e.g., 0-25 m) and then calculated the
182 ratios based upon those averages. Over the entire length of the time-series, euphotic zone
183 TON:TOP ratios varied between 34 and 130 (Fig. 2a), while TOC:TOP ratios varied between
184 450 and 1952 (Fig. 2b), and TOC:TON varied between 11 and 17 (Fig. 2c).

185 Suspended euphotic zone PON:POP ratios were generally lower than TON:TOP ratios
186 (Fig. 2, Table 1). The PON:POP ratio ranged from 7 to 140. Similarly POC:POP ratios were
187 much lower than TOC:TOP, varying from 45 to 532. The POC:PON ratio ranged between 1 and
188 19. Elemental ratios in the TOM and POM were significantly greater than the Redfield Ratio (p
189 < 0.05 ; z test) with the exception of the POC:PON ratio.

190

191 3.1. Annual patterns

192 3.1.1 Concentrations of POM and TOM

193 There were annual oscillations in POM pools in the upper 100 m (Fig. 1). TOC also showed
194 annual oscillations, however, TON concentrations were relatively constant throughout the study
195 period. The pattern of TOP was an increasing trend during early 2007 until early 2008 ($\text{TOP} =$
196 $0.0936 \times \text{decimal year} - 187.8$; $r^2 = 0.77$, $p < 0.05$). However, there were no long term sustained
197 changes in concentration of POM and TOM.

198

199 3.1.2 C:N:P ratios in POM and TOM

200 There were no discernible year-over-year trends in the POM stoichiometry (Fig. 2).
201 Amplitude of variation in the C:N:P ratios of POM was less than that in TOM. TON:TOP and
202 TOC:TOP ratios showed a decreasing trend throughout the year 2007 ($r^2 = 0.46$, $p < 0.05$),
203 which was due to an increasing trend in TOP concentration in that year (Fig. 1). There was no
204 annual trend in the TOC:TON ratio. Overall, like POM and TOM concentration patterns, there
205 were no long-term sustained changes in TOC:N:P ratios.

206

207 3.2 Seasonal variations

208 3.2.1 Concentrations of POM and TOM

209 There was greater variability in C and N pools in the 0-25 m range compared to that in
210 the 25-100 m range (Figs. 4 and 5). In the 0-25 m depth range, TOC showed an increasing trend
211 after deep mixing during the following five months before reaching a plateau ($\sim 67 \mu\text{mol kg}^{-1}$).
212 POC increased in the first month after deep mixing and then decreased during the next two
213 months and remained constant ($\sim 2 \mu\text{mol kg}^{-1}$) for the rest of the year (Fig. 4a). The pattern in
214 PON was similar to POC, while those in TON and TOC were opposite to each other during the
215 first two months after mixing and then increased until the sixth month (Fig. 4a, b). These higher
216 values of TOC and TON (observed in both 0-25 m and 25-100 m depth segments) in the sixth
217 month might be attributed to the higher occurrence of *Trichodesmium* colonies during August at
218 BATS (Orcutt et al., 2001; Singh et al., 2013). TOP and POP increased during and one month
219 after the deep mixing in the 0-25m depth range (Figs. 4c). Some of these trends (e.g., higher

220 values of TOC and TON in the sixth month) were also apparent in the 25-100 m depth range but
221 were not as prominent as in the 0-25 m depth range (Figs. 4 and 5).

222

223 3.2.2 C:N:P ratios in POM and TOM

224 TON:TOP (68 ± 9) and PON:POP (36 ± 11) values were greater than the Redfield Ratio
225 ($p < 0.05$) (Table 1). Patterns in TOC:TOP and TON:TOP ratio, and POC:POP and PON:POP
226 were similar to each other (Fig. 6a, b). TOC:TOP (983 ± 168) and POC:POP (210 ± 67) values
227 were much higher than the Redfield Ratio of 106 ($p < 0.05$). TOC:TON (15 ± 0.5) increased for
228 the two months following deep mixing and decreased until the seventh month (Fig. 6c).
229 POC:PON (6 ± 3) increased in the next month after deep mixing, but remained around the
230 Redfield Ratio throughout the year. Minimal variability in concentration and ratios in the 25-100
231 m depth range suggests confinement of the more dynamic biogeochemical processes to within
232 the mixed layer, i.e. within 0-25 m (Figs. 5 and 7).

233

234 3.2.3 N:P ratios in inorganic nutrients

235 The average $\text{NO}_3^-:\text{PO}_4^{3-}$ ratio was 25.6 ± 9.1 in the 100-500 m depth range at BATS,
236 which is greater than the Redfield Ratio (Table 1). We excluded data from the top 100 m in this
237 analysis due to low precision relative to the mean nutrient values which are at or near analytical
238 detection limits due to active biological uptake. NO_3^- and PO_4^{3-} were at their highest
239 concentrations before deep mixing and decreased immediately following the month of deepest
240 mixing and remained constant for the rest of the year (Fig. 8). The decrease in NO_3^- and PO_4^{3-}
241 concentrations was likely due to dilution with low nutrient surface water during mixing.

242

243 **3.2.4 N:P ratios in the particulate flux at 200 m**

244 The PON fluxes increased during and peaked immediately after winter mixing, while
245 POP fluxes showed elevated values before and shortly after the time of deep mixing (Fig. 8). The
246 N:P ratio of export fluxes was nearly twice that of PON:POP ratio in the suspended matter
247 (upper 100 m; Table 1).

248

249 **3.2.5 Chlorophyll *a* and phytoplankton cell abundance**

250 Chlorophyll *a* values decreased after the spring bloom that was stimulated by deep
251 mixing (Fig. 9a). *Prochlorococcus* was dominant during the oligotrophic period of the year,
252 while these were least abundant around the time of deep mixing (Fig. 9b). In contrast,
253 *Synechococcus* and picoeukaryotes were more abundant during the more productive season (Fig.
254 9c,d), and followed the annual pattern in Chlorophyll *a*. There was no discernible seasonal
255 pattern in nanoeukaryote abundance (Fig. 9e).

256

257 **4. Discussion**

258 From the approximately eight years of BATS data presented here, it is apparent that the
259 total and particulate organic matter C:N:P stoichiometries are not a long-term fixed ecosystem
260 property, but vary seasonally and deviate substantially from the canonical Redfield Ratio.
261 Observed C:N:P ratios in TOM and POM were much greater than the Redfield Ratio, averaging
262 983:68:1 and 210:36:1, respectively, for the entire dataset (Figs. 2, 4, 5).

263

264 **4.1 Connections among POM, TOM and inorganic nutrients**

Comment [MWL2]: Nearly the entire discussion has been reorganized whether within or between sections. I have not highlighted it as the entire discussion ended up highlighted.

265 Redfield hypothesized what was effectively a two-box model of nutrients shuttling
266 between particulate and dissolved form. However, there are number of different biological,
267 chemical and physical processes acting on particles as they settle through the water column.
268 Higher N:P ratios in the particulate fluxes than in the suspended matter could be due to the
269 preferential export of N or preferential remineralisation of P, but similar C:N ratios in the fluxes
270 and suspended matter would lend more support to the latter scenario (Figs. 4, 8; Table 1;
271 Monteiro and Follows, 2012). The N:P ratio of export fluxes was also generally more than twice
272 that of the dissolved $\text{NO}_3^-:\text{PO}_4^{3-}$ ratio at depth (Fig. 8c). The preferential remineralization of P
273 from settling material could potentially explain this difference, as there is little evidence for N
274 loss in this well-oxygenated region, however the advective flux of low $\text{NO}_3^-:\text{PO}_4^{3-}$ waters needs
275 to be considered. Indeed, the literature indicates that sub-euphotic waters at BATS are a mixture
276 of water originated at the north of the site, which has characteristically low $\text{NO}_3^-:\text{PO}_4^{3-}$ ratios
277 (Bates and Hansell, 2004; Singh et al., 2013). The processes of remineralization are not direct
278 from particulate to inorganic pools and indeed, cycling through the dissolved organic pool,
279 which dominates TOM, is important. One explanation for the TON:TOP ratio being greater than
280 the Redfield Ratio is that TON is less reactive than TOP and broken down mainly in the
281 subsurface layer (Letscher et al., 2013), while TOP is labile or semi-labile and both
282 remineralized and assimilated at a shallower depth (Björkman et al., 2000). Consequently, TOP
283 has faster turnover times (Clark et al., 1998). In contrast to this interpretation, our observations
284 suggest that TON and TOP values increase slightly with depth suggesting a net (i.e.,
285 remineralization exceeding assimilation) flow of material from the particulate organic pool to the
286 dissolved organic pool for both elements (comparing data in Figs. 4 and 5).

287 Our results on the TON:TOP ratio have important implications in ocean biogeochemistry
288 of oligotrophic waters where DON and DOP concentrations in the sunlit layers exceed the
289 concentration of inorganic nutrients by an order of magnitude. Dissolved organic pools are
290 essential in sustaining phytoplankton growth in these regions (Church et al., 2002; Williams and
291 Follows, 1998). Nutrient levels decide phytoplankton growth and their stoichiometry
292 (Klausmeier et al., 2004), hence TON:TOP in the oligotrophic regions might determine optimal
293 N:P stoichiometry of phytoplankton rather than the inorganic pools alone.

294

295 **4.2 Linkages of concentrations and ratios of POM and TOM to chlorophyll *a* and** 296 **phytoplankton**

297 We hypothesize that C:N:P ratios in the aggregated phytoplankton community itself
298 changes the elemental stoichiometry of the POM and TOM pools. The C:N:P ratio is different in
299 different phytoplankton communities and their biological uptake and degradation could
300 potentially change the elemental stoichiometry of the particulate and dissolved organic matter.
301 The C:N:P ratio varies geographically and its pattern correlates with global variations in
302 temperature, overall nutrient concentrations and phytoplankton functional groups. These
303 latitudinal patterns in the C:N:P ratio have been attributed to changes in phytoplankton
304 community as polar (colder) regions have a high abundance of diatoms with low N:P and C:P
305 ratios, in contrast to the directly measured high elemental ratios in cyanobacteria from warmer
306 regions (Martiny et al., 2013). So how and why does C:N:P ratio vary in phytoplankton
307 communities? Two mechanisms could explain variability in the C:N:P ratios in a phytoplankton
308 community. The first mechanism suggests that the taxonomic composition of a phytoplankton
309 community influences its elemental composition. Elemental ratios inside a cell are controlled by

310 growth strategies (Klausmeier et al., 2004) . Studies have reported low C:P and N:P ratios in fast
311 growing diatoms (e.g., Price, 2005), whereas slower growing cyanobacteria have C:P and N:P
312 ratios higher than the Redfield Ratio (Bertilsson et al., 2003; Martiny et al., 2013). More
313 precisely, it is not so much the growth rate that determines the difference, but the machinery
314 invested in nutrient acquisition versus protein production.

315 The second mechanism links the nutrient supply ratio to a taxonomically ‘hard-wired’
316 cellular elemental ratio (Rhee, 1978). Chlorophyll *a* values were anti-correlated with TOC
317 values ($r^2 = 0.76, p < 0.05$). The gradual increase in Chlorophyll *a* during the four months before
318 deep mixing is due to similar increase in MLD before deep mixing (Fig. 3), which suggests that
319 there may be enhanced nutrient flux into the upper layer well before deep mixing (e.g., Fawcett
320 et al. 2014). *Prochlorococcus* and *Synechococcus* profiles were correlated to each other in the
321 first seven months from the point of deepest mixing ($r^2 = 0.58, p < 0.05$) and there was no
322 relation in the rest of the year in the 0-25 m depth range. Furthermore, *Synechococcus* cell
323 abundance was correlated with POC ($r^2 = 0.67 p < 0.05$), PON ($r^2 = 0.47 p < 0.05$), POP ($r^2 =$
324 $0.29 p < 0.05$) and anti-correlated with TOC values ($r^2 = 0.72 p < 0.05$) in the 0-25 m depth
325 range. *Synechococcus* is more abundant during the more productive season whereas
326 *Prochlorococcus* is dominant during the highly oligotrophic part of the year. Such patterns are
327 typically observed in many parts of the ocean. The seasonal pattern of picoeukaryote abundance
328 was similar to that of *Synechococcus* ($r^2 = 0.58 p < 0.05$) and Chlorophyll *a* ($r^2 = 0.81 p < 0.05$).
329 POC:PON:POP ratios in *Prochlorococcus*, *Synechococcus* and picoeukaryote are 234:33:1,
330 181:33:1 and 118:15:1, respectively at the BATS site (Martiny et al., 2013 and Lomas et al.,
331 unpublished data), which clearly suggests imprints of a mixture of *Prochlorococcus*,
332 *Synechococcus* on the observed POM stoichiometry presented in Table 1. Biomass of

333 *Prochlorococcus*, *Synechococcus* and picoeukaryotes together contributes ~40% to the POC pool
334 (Casey et al. 2013) and ~75% to the PON pool (Fawcett et al. 2011), with major contributions
335 from each group varying seasonally. Hence, variability in biological parameters could potentially
336 explain a significant fraction of the variability in the POM and TOM ratios, but not all of it. So
337 what else drives the variability in the C:N:P ratios?

338 We analysed trends in the TON:TOP and TOC:TOP ratios for December 2006 to January
339 2008 data along with phytoplankton cell abundances for the top 100 m BATS data. Since the
340 variation in TON:TOP and TOC:TOP were due to an increasing trend in TOP, we correlated
341 TOP concentrations with a lag of three months (there is a time lag between phytoplankton and
342 elemental abundance as observed by Singh et al., 2013) in phytoplankton cell abundances (data
343 during September 2006 to November 2007; Fig. 10a). We observed significant anti-correlation
344 ($r^2 = 0.61$, $p < 0.001$) between nanoeukaryotes and TOP but the data did not correlate with other
345 phytoplankton groups (Fig. 10a). In the paucity of elemental composition data on
346 nanoeukaryotes, we hypothesize that these cells have a high requirement for P and are potentially
347 meeting that requirement by assimilating TOP.

348 We further analysed this increasing trend in the TOP concentration with climate indices.
349 The Arctic Oscillation is a major climatic phenomenon in the North Atlantic Ocean (Thompson
350 and Wallace, 1999). Positive trends in the Arctic Oscillation lead to higher temperatures,
351 advanced spring, and increased CO₂. This could lead to enhanced uptake of CO₂ during spring as
352 has been found in terrestrial systems (Schaefer et al., 2005). Higher build-up of organic matter
353 would require more P and hence we correlated TOP concentration with monthly Arctic
354 Oscillation index with a lag of a year (monthly Arctic Oscillation indices are from November
355 2005 to December 2006, because there is a lag of one year before climatic oscillations in the

356 North Atlantic show its impact on surface biogeochemistry; Fromentin and Planque, 1996). We
357 observed a significant correlation ($r^2 = 0.46$, $p < 0.01$) between the Arctic Oscillation and TOP
358 concentrations (Fig. 10b). Since variations in phytoplankton cell abundances and climate
359 variability could not explain all the variation in the elemental stoichiometry, other mechanisms
360 are yet to be identified to explain the observed variability in the elemental stoichiometry.

361

362 **4.3 Role of DOM in microbial carbon export**

363 Many biogeochemical model estimates of export production assume Redfield
364 stoichiometry in export fluxes but a non-Redfieldian approach has gained appreciation recently
365 (Letscher and Moore, 2015). Export production is estimated to be 3-4 mol C m⁻² yr⁻¹ in the
366 BATS region (Jenkins, 1982; Emerson, 2014), which requires more nutrient input than
367 observations suggest (Williams and Follows, 1998). A possible mechanism to sustain such
368 export production is the supply of DOM to the sunlit layer.

369 DOM consists of complex compounds whose chemical characterization is incomplete,
370 but it is evident that DOM elemental stoichiometry differs drastically from the Redfield Ratio.
371 Differential production and degradation of DON and DOP with lifetimes comparable to the gyre
372 circulation could potentially change the overall stoichiometry of nutrient supply (Voss and
373 Hietanen, 2013). Preferential degradation of DOP rather than DON expands the niche of
374 diazotrophs beyond that created by subsurface denitrification. Diazotrophs can quickly utilize
375 recycled DOP (Dyhrman et al., 2006). Simultaneously, these diazotrophs release DON
376 (Mulholland, 2007), which can be used by other phytoplankton, but this DON likely has
377 associated DOP. In the P stressed Sargasso Sea, DOP contributes up to 50% of P demand for
378 primary production (Lomas et al. 2010) and up to 70% to the exported POP (Roussenov et al.,

379 2006; Torres-Valdés et al., 2009). Indeed, a 1-D biogeochemical model for BATS that included
380 an explicit DOP pool and a generic DOM pool significantly improved the capture of natural
381 variability in both particulate (suspended and exported) and dissolved (organic and inorganic)
382 pools (Salihoglu et al. 2007). These model results, as well as others connecting DOP cycling to
383 particulate P export (e.g., Roussenov et al. 2007), suggest a strong need for direct rate
384 measurements of DOM production and assimilation (e.g., Mahaffey et al. 2014).

385

386 **Conclusion**

387 Our time-series analysis suggests temporal and depth variability in the C:N:P ratio in the
388 Sargasso Sea. C:N:P ratios in the TOM were significantly higher than the canonical Redfield
389 Ratio, while C:N was similar to the Redfield Ratio in the POM. We observed seasonal variability
390 in stoichiometry but on average the TOC:TON:TOP ratio was 983:68:1 and the POC:PON:POP
391 was 210:36:1. **Seasonal variation in POM stoichiometry** appears to be largely driven by the
392 growth of *Synechococcus* during winter mixing, while flourishing of *Prochlorococcus* cells
393 during the oligotrophic period (fall) could also explain some variability in the stoichiometry. **The**
394 **C:N:P ratio in *Prochlorococcus* cells resembles observed mean POC:PON:POP ratio at BATS**
395 **(210:36:1)**. The N:P ratio in subsurface inorganic nutrients was also greater (N:P = 26) than the
396 Redfield Ratio in this region. We observed a significant decreasing trend in TON:TOP and
397 TOC:TOP during 2007, which was due to an increase in TOP concentration and could have been
398 partly driven by the Arctic Oscillation and a decrease in the relative abundance of
399 nanoeukaryotes. Other causes for the observed variations in the elemental stoichiometry need to
400 be explored; however, this elemental stoichiometry analysis may improve biogeochemical
401 models, which have hitherto assumed Redfield stoichiometry to estimate export fluxes.

402

403

404

405 **Acknowledgments**

406 We sincerely thank the research technicians, captains and crew of BATS cruises for their
407 contribution to the data, and the National Science Foundation Chemical and Biological
408 Oceanography Programs for continued support of the BATS program through the following
409 awards: OCE 88–01089, OCE 93–01950, OCE 9617795, OCE 0326885, OCE 0752366, and
410 OCE-0801991. This work was financially supported by Centre of Excellence (CoE) funded by
411 Nippon Foundation (NF)–Partnership for Observations of the Global Ocean (POGO) and a grant
412 (CP1213) of the Cluster of Excellence 80 ‘The Future Ocean’ to AS.

413

414

- 415 **References**
- 416 Arrigo, K. R.: Marine microorganisms and global nutrient cycles, *Nature*, 437, 349–355,
417 doi:10.1038/nature04158, 2005.
- 418 Arrigo, K. R., Robinson, D. H., Worthen, D. L., Dunbar, R. B., DiTullio, G. R., VanWoert, M.
419 and Lizotte, M. P.: Phytoplankton Community Structure and the Drawdown of Nutrients and
420 CO₂ in the Southern Ocean, *Science*, 283, 365–367, doi:10.1126/science.283.5400.365, 1999.
- 421 Bates, N. R. and Hansell, D. A.: Temporal variability of excess nitrate in the subtropical mode
422 water of the North Atlantic Ocean, *Mar. Chem.*, 84, 225–241,
423 doi:10.1016/j.marchem.2003.08.003, 2004.
- 424 Bertilsson, S., Berglund, O., Karl, D. M. and Chisholm, S. W.: Elemental composition of marine
425 *Prochlorococcus* and *Synechococcus*: Implications for the ecological stoichiometry of the sea,
426 *Limnol. Oceanogr.*, 48(5), 1721–1731, 2003.
- 427 Björkman, K., Thomson-Bulldis, A. L. and Karl, D. M.: Phosphorus dynamics in the North
428 Pacific subtropical gyre, *Aquat. Microb. Ecol.*, 22, 185–198, 2000.
- 429 Carlson, C. A., Morris, R., Parsons, R., Treusch, A. H., Giovannoni, S. J. and Vergin, K.:
430 Seasonal dynamics of SAR11 populations in the euphotic and mesopelagic zones of the
431 northwestern Sargasso Sea, *ISME J.*, 3(3), 283–295, 2009.
- 432 Carlson, C. A., Hansell, D. A., Nelson, N. B., Siegel, D. A., Smethie, W. M., Khatiwala, S.,
433 Meyers, M. M. and Halewood, E.: Dissolved organic carbon export and subsequent
434 remineralization in the mesopelagic and bathypelagic realms of the North Atlantic basin, *Deep-
435 Sea Res. II*, 57, 1433–1445, doi:10.1016/j.dsr2.2010.02.013, 2010.
- 436 Casey, J.R., Aucan, J.P., Goldberg, S.R., Lomas, M.W. 2013. Changes in partitioning of carbon
437 amongst photosynthetic pico- and nano-plankton groups in the Sargasso Sea in response to
438 changes in the North Atlantic Oscillation. *Deep Sea Res. II*, 93:58-70.
439
- 440 Church, M. J., Ducklow, H. W. and Karl, D. M.: Multiyear increases in dissolved organic matter
441 inventories at Station ALOHA in the North Pacific Subtropical Gyre, *Limnol. Oceanogr.*, 47(1),
442 1–10, 2002.
- 443 Clark, L. L., Ingall, E. D. and Benner, R.: Marine phosphorus is selectively remineralized,
444 *Nature*, 393(6684), 426, doi:10.1038/30881, 1998.
- 445 Copin-Montegut, C. and Copin-Montegut, G.: Stoichiometry of carbon, nitrogen, and
446 phosphorus in marine particulate matter, *Deep-Sea Res. II*, 30(1), 31–46, 1983.
- 447 Dore, J. E., Houlihan, T., Hebel, D. V., Tien, G. A., Tupas, L. M. and Karl, D. M.: Freezing as a
448 method of sample preservation for the analysis of dissolved inorganic nutrients in seawater, *Mar.
449 Chem.*, 53, 173–185, 1996.

Comment [MWL3]: A number of relevant references added in conjunction with the rewrite of the discussion.

450 Dyhrman, S. T., Chappel, P. D., Haley, S. T., Moffet, J. W., Orchard, E. D., Waterbury, J. B. and
451 Webb, J. B.: Phosphonate utilization by the globally important marine diazotroph
452 *Trichodesmium*, *Nature*, 439, 68–71, doi:10.1038/nature04203, 2006.

453 Emerson, S.: Annual net community production and the biological carbon flux in the ocean,
454 *Glob. Biogeochem. Cycles*, 28, 14–28, doi:10.1002/2013GB004680, 2014.

455 Falkowski, P. G. and Raven, J. A.: *Aquatic photosynthesis*, Blackwell Science, Oxford, UK.,
456 1997.

457 Fawcett, S.E., Lomas, M.W., Casey, J.R., Ward, B.B., Sigman, D.M. 2011. Assimilation of
458 upwelled nitrate by small eukaryotes in the Sargasso Sea. *Nature Geoscience*, 4:717-722.

459 Fawcett, S.E., Lomas, M.W., Ward, B.B., Sigman, D.M. 2014. The counterintuitive effect of
460 summer-to-fall mixed layer deepening on eukaryotic new production in the Sargasso Sea. *Glob.*
461 *Biogeochem. Cycles*, 10.1002/2013GB004579.

462 Fromentin, J.-M. and Planque, B.: Calanus and environment in the eastern North Atlantic. II.
463 Influence of the North Atlantic Oscillation on *C. finmarchicus* and *C. helgolandicus*, *Mar. Ecol.*
464 *Prog. Ser.*, 134, 111–118, 1996.

465 Gardner, W. D., Chung, S. P., Richardson, M. J. and Walsh, I. D.: The oceanic mixed-layer
466 pump, *Deep-Sea Res. II*, 42(2-3), 757–775, 1995.

467 Geider, R. J. and La Roche, J.: Redfield revisited: variability of C:N:P in marine microalgae and
468 its biochemical basis, *Eur. J. Phycol.*, 37, 1–17, doi:10.1017/S0967026201003456, 2002.

469 Goldman, J. C., McCarthy, J. J. and Peavey, D. G.: Growth rate influence on the chemical
470 composition of phytoplankton in oceanic waters, *Nature*, 279, 210–215, 1979.

471 Gruber, N. and Deutsch, C. A.: Redfield’s evolving legacy, *Nat. Geosci.*, 7(12), 853–855, 2014.

472 Gruber, N. and Sarmiento, J. L.: Global patterns of marine nitrogen fixation and Denitrification,
473 *Glob. Biogeochem. Cycles*, 11(2), 235–266, 1997.

474 Heldal, M., Scanlal, D. J., Norland, S., Thingstad, F. and Mann, N. H.: Elemental composition of
475 single cells of various strains of marine *Prochlorococcus* and *Synechococcus* using X-ray
476 microanalysis, *Limnol. Oceanogr.*, 48(5), 1732–1743, 2003.

477 Heukelem, L. V. and Thoams, C. S.: Computer-assisted high-performance liquid
478 chromatography method development with applications to the isolation and analysis of
479 phytoplankton pigments, *J. Chromatogr. A*, 910, 31–49, 2001.

480 Jenkins, W. J.: Oxygen utilization rates in the North Atlantic subtropical gyre and primary
481 production in oligotrophic systems, *Nature*, 300(5889), 246–248, 1982.

482 Karl, D. M. and Tein, G.: Temporal variability in dissolved phosphorus concentrations in the
483 subtropical North Pacific Ocean, *Mar. Chem.*, 56, 77–96, 1997.

484 Karl, D. M., Letelier, R., Hebel, D. V., Bird, D. F. and Winn, C. D.: *Trichodesmium* blooms and
485 new nitrogen in the north Pacific gyre, in *Marine Pelagic Cyanobacteria: Trichodesmium and*
486 *other Diazotrophs*, pp. 219–237, Springer, Netherlands., 1992.

487 Karl, D. M., Björkman, K. M., Dore, J. E., Fujieki, L., Hebel, D. V., Houlihan, T., Letelier, R.
488 M. and Tupas, L. M.: Ecological nitrogen-to-phosphorus stoichiometry at station ALOHA,
489 *Deep-Sea Res. II*, 48, 1529–1566, 2001.

490 Klausmeier, C. A., Litchman, E., Daufresne, T. and Levin, S. A.: Optimal nitrogen-to-
491 phosphorus stoichiometry of phytoplankton, *Nature*, 429, 171–174, 2004.

492 Lenton, T. M. and Watson, A. J.: Redfield revisited 1. Regulation of nitrate, phosphate, and
493 oxygen in the ocean, *Glob. Biogeochem. Cycles*, 14(1), 225–248, 2000.

494 Letelier, R. M. and Karl, D. M.: Role of *Trichodesmium* spp. in the productivity of the
495 subtropical North Pacific Ocean, *Mar. Ecol. Prog. Ser.*, 133, 263–273, 1996.

496 Letscher, R. T. and Moore, J. K.: Preferential remineralization of dissolved organic phosphorus
497 and non-Redfield DOM dynamics in the global ocean: Impacts on marine productivity, nitrogen
498 fixation, and carbon export, *Glob. Biogeochem. Cycles*, 29(3), 325–340, doi:10.1002/
499 2014GB004904, 2015.

500 Letscher, R. T., Hansell, D. A., Carlson, C. A., Lumpkin, R. and Knapp, A. N.: Dissolved
501 organic nitrogen in the global surface ocean: Distribution and fate, *Glob. Biogeochem. Cycles*,
502 27, 1–13, doi:10.1029/2012GB004449, 2013.

503 Lomas, M. W., Burke, A. L., Lomas, D. A., Bell, D. W., Shen, C., Dyhrman, S. T. and
504 Ammerman, J. W.: Sargasso Sea phosphorus biogeochemistry: an important role for dissolved
505 organic phosphorus (DOP), *Biogeosciences*, 7, 695–710, 2010.

506 Lomas, M. W., Bates, N. R., Johnson, R. J., Knap, A. H., Steinberg, D. K. and Carlson, C. A.:
507 Two decades and counting: 24-years of sustained open ocean biogeochemical measurements in
508 the Sargasso Sea, *Deep-Sea Res. II*, 93, 16–32, 2013.

509 Mahaffey, C., Michaels, A. F. and Capone, D. G.: The conundrum of marine nitrogen fixation,
510 *Am. J. Sci.*, 305, 546–595, 2005.

511
512 Mahaffey, C., Reynolds, S., Davis, C. E., and Lohan, M. C. 2014. Alkaline phosphatase activity
513 in the subtropical ocean: insights from nutrient, dust and trace metal addition experiments. *Front.*
514 *Mar. Sci.* 1:73. doi: 10.3389/fmars.2014.00073
515

516 Martiny, A. C., Pham, C. T. A., Primeau, F. W., Vrugt, J. A., Moore, J. K., Levin, S. A. and
517 Lomas, M. W.: Strong latitudinal patterns in the elemental ratios of marine plankton and organic
518 matter, *Nat. Geosci.*, 6, 279–283, doi:10.1038/NGEO1757, 2013.

519 Mills, M. M. and Arrigo, K. R.: Magnitude of oceanic nitrogen fixation influenced by the
520 nutrient uptake ratio of phytoplankton, *Nat. Geosci.*, 3, 412–416, doi:10.1038/NGEO856, 2010.

- 521 Monteiro, F. M. and Follows, M. J.: On nitrogen fixation and preferential remineralization of
522 phosphorus, *Geophys. Res. Lett.*, 39, L06607, doi:10.1029/2012GL050897, 2012.
- 523 Moore, C. M., Mills, M. M., Arrigo, K. R., Berman-Frank, I., Bopp, L., Boyd, P. W., Galbraith,
524 E. D., Guieu, C., Jaccard, S. L., Jickells, T. D., La Roche, J., Lenton, T. M., Mahowald, N.,
525 Marañón, E., Marinov, I., Moore, J. K., Nakatsuka, T., Oschlies, A., Saito, M. A., Thingstad, T.
526 F., Tsuda, A. and Ulloa, A.: Processes and patterns of oceanic nutrient limitation, *Nat. Geosci.*, 6,
527 701–710, doi:10.1038/NGEO1765, 2013.
- 528 Mulholland, M. R.: The fate of nitrogen fixed by diazotrophs in the ocean, *Biogeosciences*, 4,
529 31–57, 2007.
- 530 Orcutt, K. M., Lipschultz, F., Gundersen, K., Arimoto, R., Michaels, A. F., Knap, A. H. and
531 Gallon, J. R.: A seasonal study of the significance of N₂ fixation by *Trichodesmium* spp. at the
532 Bermuda Atlantic Time-series Study (BATS) site, *Deep-Sea Res. II*, 48, 1583–1608, 2001.
- 533 Pahlow, M. and Riebesell, U.: Temporal Trends in Deep Ocean Redfield Ratios, *Science*, 287,
534 831–833, doi:10.1126/science.287.5454.831, 2000.
- 535 Price, N. M.: The elemental stoichiometry and composition of an iron-limited diatom, *Limnol.*
536 *Oceanogr.*, 50(4), 1159–1171, 2005.
- 537 Quigg, A., Finkel, Z. V., Irwin, A. J., Rosenthal, Y., Ho, T.-Y., Reinfelder, J. R., Schofield, O.,
538 Morel, F. M. M. and Falkowski, P. G.: The evolutionary inheritance of elemental stoichiometry
539 in marine phytoplankton, *Nature*, 425, 291–294, 2003.
- 540 Redfield, A. C.: On the proportions of organic derivatives in seawater and their relation to the
541 composition of plankton, in James Johnstone Memorial Volume, pp. 176–192, university press
542 of liverpool, Liverpool, UK., 1934.
- 543 Redfield, A. C.: The biological control of chemical factors in the environment, *Am. Sci.*, 46,
544 205–221, 1958.
- 545 Rhee, G.-Y.: Effects of N:P atomic ratios and nitrate limitation on algal growth, cell
546 composition, and nitrate uptake, *Limnol. Oceanogr.*, 23(1), 10–25, 1978.
- 547 Roussenov, V. M., Williams, R. G., Mahaffey, C. and Wolff, G. A.: Does the transport of
548 dissolved organic nutrients affect export production in the Atlantic Ocean?, *Glob. Biogeochem.*
549 *Cycles*, 20(GB3002), doi:10.1029/2005GB002510, 2006.
- 550 Salihoglu, B., Garçon, V., Oschlies, A., Lomas, M.W. 2007. Influence of nutrient
551 remineralization and utilization stoichiometry on phytoplankton species and carbon export: A
552 modeling study at BATS. *Deep Sea Res. I*, 55: 73-107.
- 553 Sañudo-Wilhelmy, S. A., Kustka, A. B., Gobler, C. J., Hutchins, D. A., Yang, M., Lwiza, K.,
554 Burns, J., Capone, D. G., Raven, J. A. and Carpenter, E. J.: Phosphorus limitation of nitrogen
555 fixation by *Trichodesmium* in the central Atlantic Ocean, *Nature*, 411, 66–69, 2001.

556 Sañudo-Wilhelmy, S. A., Tovar-Sanchez, A., Fu, F.-X., Capone, D. G. and Hutchins, D. A.: The
557 impact of surface-adsorbed phosphorus on phytoplankton Redfield stoichiometry, *Nature*, 432,
558 897–901, 2004.

559 Schaefer, K., Denning, A. S. and Leonard, O.: The winter Arctic Oscillation, the timing of
560 spring, and carbon fluxes in the Northern Hemisphere, *Glob. Biogeochem. Cycles*, 19, GB3017,
561 doi:10.1029/2004GB002336, 2005.

562 Siegel, D. A., Westberry, T. K., O'Brien, M. C., Nelson, N. B., Michaels, A. F., Morrison, J. R.,
563 Schott, A., Caporelli, E. A., Sorenson, J. C., Maritorena, S., Garver, S. A., Brody, E. A., Ubante,
564 J. and Hammer, M. A.: Bio-optical modeling of primary production on regional scales: the
565 Bermuda BioOptics project, *Deep-Sea Res. II*, 48, 1865–1896, 2001.

566 Sigman, D. M. and Boyle, E. A.: Glacial/interglacial variations in atmospheric carbon dioxide,
567 *Nature*, 407, 859–869, 2000.

568 Singh, A., Lomas, M. W. and Bates, N. R.: Revisiting N₂ fixation in the North Atlantic Ocean:
569 significance of deviations in Redfield Ratio, atmospheric deposition and climate variability,
570 *Deep-Sea Res. II*, 93, 148–158, doi:10.1016/j.dsr2.2013.04.008, 2013.

571 Steinberg, D. K., Carlson, C. A., Bates, N. R., Johnson, R. J., Michaels, A. F. and Knap, A. H.:
572 Overview of the US JGOFS Bermuda Atlantic Time-series Study (BATS): a decade-scale look at
573 ocean biology and biogeochemistry, *Deep-Sea Res. II*, 48, 1405–1447, 2001.

574 Teng, Y.-C., Primeau, F. W., Moore, J. K., Lomas, M. W. and Martiny, A. C.: Global-scale
575 variations of the ratios of carbon to phosphorus in exported marine organic matter, *Nat. Geosci.*,
576 7, 895–898, doi:10.1038/NGEO2303, 2014.

577 Thompson, D. W. J. and Wallace, J. M.: The Arctic Oscillation signature in wintertime
578 geopotential height and temperature fields, *Geophys. Res. Lett.*, 25(9), 1297–1300, 1999.

579 Torres-Valdés, S., Roussinov, V. M., Sanders, R., Reynolds, S., Pan, X., Mather, R., Landolfi,
580 A., Woff, G. A., Achterberg, E. P. and Williams, R. G.: Distribution of dissolved organic
581 nutrients and their effect on export production over the Atlantic Ocean, *Glob. Biogeochem.*
582 *Cycles*, 23, GB4019, doi:10.1029/2008GB003389, 2009.

583 Tyrrell, T.: The relative influences of nitrogen and phosphorus on oceanic primary production,
584 *Nature*, 400, 525–531, 1999.

585 Vidal, M., Durate, C. M. and Agustí, S.: Dissolved organic nitrogen and phosphorus pools and
586 fluxes in the central Atlantic Ocean, *Limnol. Oceanogr.*, 44(1), 106–115, 1999.

587 Voss, M. and Hietanen, S.: The depths of nitrogen cycling, *Nature*, 493, 616–618, 2013.

588 Weber, T. S. and Deutsch, C. A.: Ocean nutrient ratios governed by plankton biogeography,
589 *Nature*, 467, 550–554, doi:10.1038/nature09403, 2010.

590 Williams, R. G. and Follows, M. J.: The Ekman transfer of nutrients and maintenance of new
591 production over the North Atlantic, *Deep-Sea Res. I*, 45, 461–489, 1998.

592 Wu, J., Sunda, W., Boyle, E. A. and Karl, D. M.: Phosphate Depletion in the Western North
593 Atlantic Ocean, *Science*, 289, 759–762, doi:10.1126/science.289.5480.759, 2000.

594 Zamora, L. M., Landolfi, A., Oschlies, A., Hansell, D. A., Dietze, H. and Dentener, F.:
595 Atmospheric deposition of nutrients and excess N formation in the North Atlantic,
596 *Biogeosciences*, 7, 777–793, 2010.

597

598

599

600

601

602

603 **Table 1.** Average concentration ($\mu\text{mol kg}^{-1}$), molar ratio of various biogeochemical parameters
 604 and particle fluxes ($\text{mmol m}^{-2} \text{d}^{-1}$) from the BATS data presented in Fig. 1.

| <i>Concentration (C) in the upper 100 m</i> | | | |
|--|-----------------------|--------------------------------|-----------------------|
| Parameter | $C \pm \sigma^*$ | no of samples | Sampling period |
| TOC | 63.81 ± 2.86 | 714 | Jan 2004 - Dec 2011 |
| TON | 4.43 ± 0.50 | 712 | Jan 2004 - Dec 2011 |
| TOP | 0.07 ± 0.03 | 547 | Jun 2004 - Nov 2011 |
| POC | 2.36 ± 1.14 | 844 | Jan 2004 - April 2012 |
| PON | 0.40 ± 0.19 | 845 | Jan 2004 - April 2012 |
| POP | 0.01 ± 0.01 | 696 | Jan 2004 - April 2012 |
| <i>Ratio (R)[†] in the upper 100 m</i> | | | |
| Parameter | $R \pm \sigma$ | no of data points [‡] | Sampling period |
| TOC:TON | 15 ± 0.5 | 86 | Jul 2004 - Dec 2011 |
| POC:PON | 6 ± 3 | 95 | Jan 2004 - Apr 2012 |
| TON:TOP | 68 ± 9 | 77 | Jul 2004 - Nov 2011 |
| PON:POP | 36 ± 11 | 88 | Jan 2004 - Apr 2012 |
| TOC:TOP | 983 ± 168 | 78 | Jul 2004 - Nov 2011 |
| POC:POP | 210 ± 67 | 88 | Jan 2004 - Apr 2012 |
| <i>Inorganic nutrient stoichiometry in 100-500 m</i> | | | |
| Parameter | (C or R) $\pm \sigma$ | no of data points | Sampling period |
| NO_3^- | 2.74 ± 2.40 | 3425 | Oct 1988 - July 2012 |
| PO_4^{3-} | 0.11 ± 0.13 | 3405 | Oct 1988 - July 2012 |
| $\text{NO}_3^-:\text{PO}_4^{3-}$ | 25.6 ± 9.1 | 2415 | Oct 1988 - July 2012 |
| <i>Particle fluxes at 200 m</i> | | | |
| Parameter | $C \pm \sigma$ | no of samples | Sampling period |
| C | 1.68 ± 1.07 | 254 | Jan 1989 - Dec 2011 |
| N | 0.23 ± 0.16 | 254 | Jan 1989 - Dec 2011 |
| P | 0.008 ± 0.014 | 64 | Oct 2005 - Dec 2011 |
| <i>Ratio in particle fluxes at 200 m</i> | | | |
| Parameter | $R \pm \sigma$ | no of data points | Sampling period |
| N:P | 57 ± 46 | 61 | Oct 2005 - Dec 2011 |
| C:P | 287 ± 269 | 62 | Oct 2005 - Dec 2011 |
| C:N | 7.9 ± 2.8 | 252 | Jan 1989 - Dec 2011 |

605 * σ is standard deviation of the samples mentioned in next the column. [†]Ratios and their standard
 606 deviations are derived from the monthly mean values ([‡]one datum would be mean of many
 607 values of concentration for a particular month) of concentration in the upper 100 m.
 608
 609
 610
 611

612 **Figure Captions:**

613 **Fig. 1.** Monthly BATS data on C, N and P in total and particulate organic matter in top 100 m
614 during Jan 2004 to April 2012.

615

616 **Fig. 2.** Monthly stoichiometry during 2004-2010 at 0-100 m. Solid lines are three month running
617 means. Error bars are 1σ standard deviations from the mean values.

618

619 **Fig. 3.** Mixed layer depth (MLD) during the sampling period at BATS site.

620

621 **Fig. 4.** Box/whisker plot comparing the annual concentrations of total (open bars) and particulate
622 organic matter (filled bars) relative to the deep mixing in 0-25 m depth at BATS (data used from
623 January 2005 - December 2011). Bottom and top of the box define the 25% and 75% data
624 distribution, and the 'error' bars define the 5% and 95% data distribution. The dark gray vertical
625 bar represents the period of deep mixing (DM) for each year.

626

627 **Fig. 5.** Box/whisker plot comparing the annual concentrations of total (open bars) and particulate
628 (filled bars) matter relative to the deep mixing at 25-100 m depth (data used from January 2005 -
629 December 2011). All else as in Figure 4.

630

631 **Fig. 6.** Box/whisker plot comparing the annual ratios of elemental stoichiometry relative to the
632 deep mixing at 0-25 m depth (data used from January 2005 - December 2011). All else as in
633 Figure 4.

634

635 **Fig. 7.** Box/whisker plot comparing the annual ratios of elemental stoichiometry relative to the
636 deep mixing at 25-100 m depth (data used from January 2005 - December 2011). The gray bar
637 represents the period of deep mixing (DM) for each year. All else as in Figure 4.

638

639 **Fig. 8.** Box/whisker plot comparing the annual variation of NO_3^- and PO_4^{3-} and their ratio
640 relative to the deep mixing at 100-500 m depth (data used from January 2005 - December 2011).
641 The gray bar represents the period of deep mixing (DM) for each year. All else as in Figure 4.

642

643 **Fig. 9.** Box/whisker plot comparing the annual variation in Chlorophyll *a* and cell counts for
644 *Prochlorococcus*, *Synechococcus*, Picoeukaryotes, and Nanoeukaryotes relative to the deep
645 mixing in 0-25 m depth at BATS (data used from January 2005 - December 2011). The gray bar
646 represents the period of deep mixing for each year. All else as in Figure 4.

647

648 **Fig. 10.** Relationship between TOP (Dec 2006 - Jan 2008) and (a) cell abundances (natural log
649 transformed) of *Prochlorococcus*, *Synechococcus*, Picoeukaryotes and Nanoeukaryotes during
650 Sep 2006 - Nov 2007. Among cell abundances, only Nanoeukaryotes showed a significant
651 relationship with TOP ($r^2 = 0.61$, $p < 0.001$) (b) Relationship between TOP and Arctic
652 Oscillation index during Nov 2005 - Dec 2006 ($r^2 = 0.46$, $p < 0.01$).

653

654

655

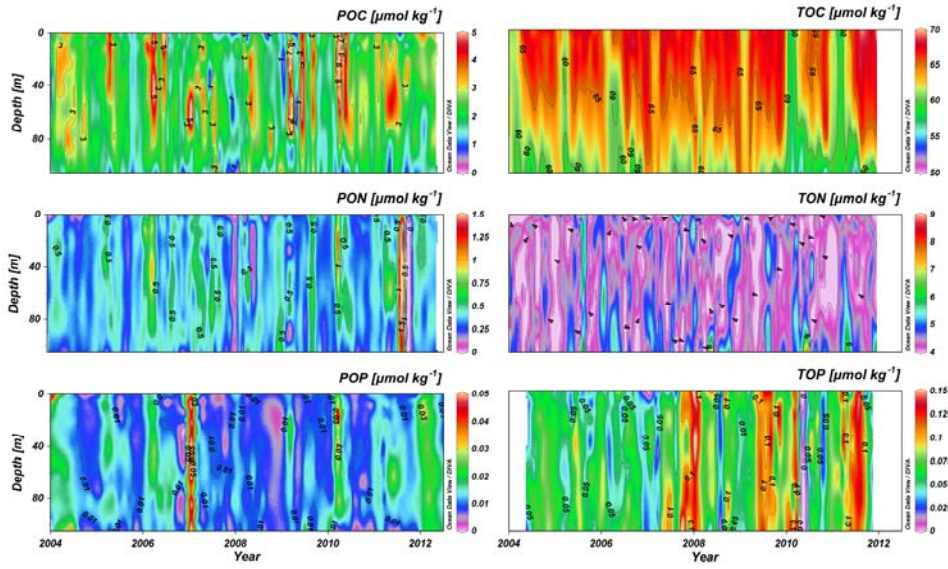
656

657

658

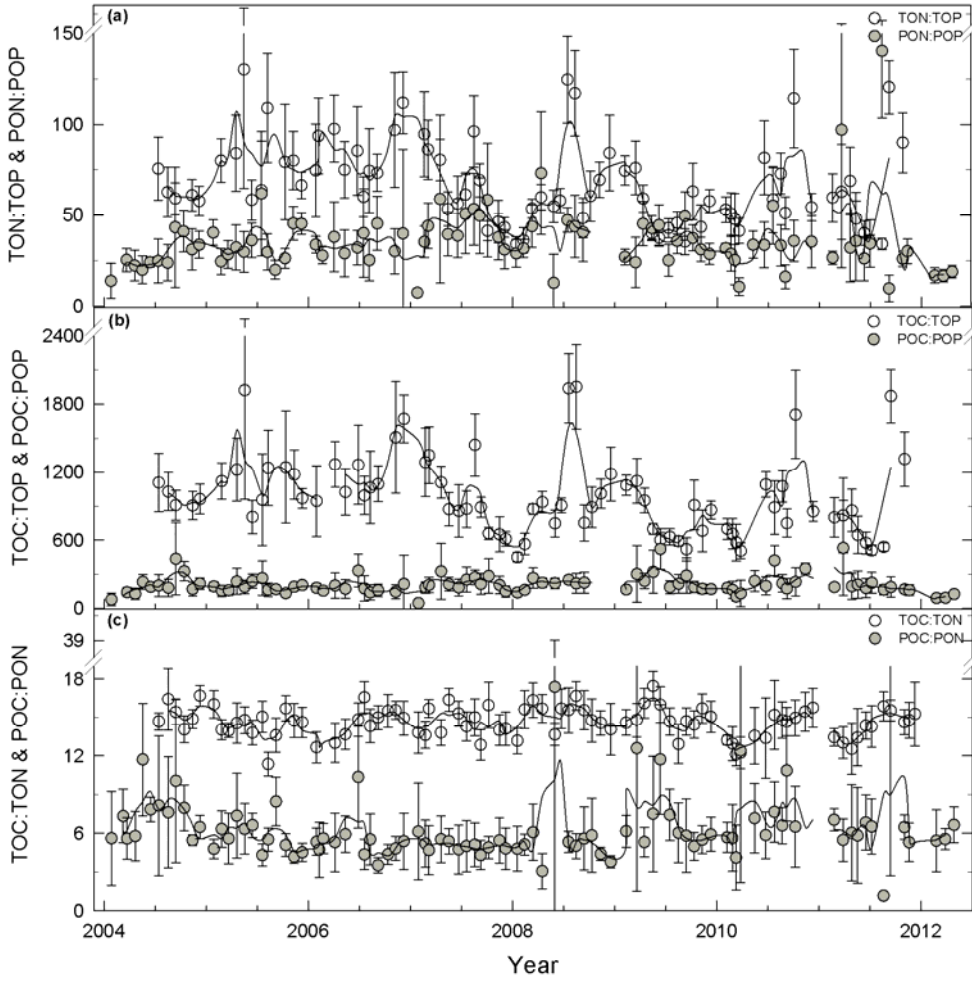
659 **Fig.1**

Comment [MWL4]: Color figure to improve value.



660
661
662
663
664
665
666
667
668
669
670
671
672

673 **Fig. 2**



674

675

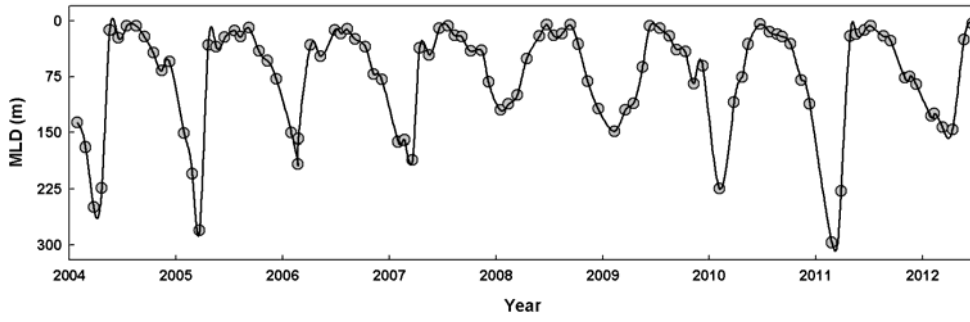
676

677

678

679

680 Fig. 3



681

682

683

684

685

686

687

688

689

690

691

692

693

694

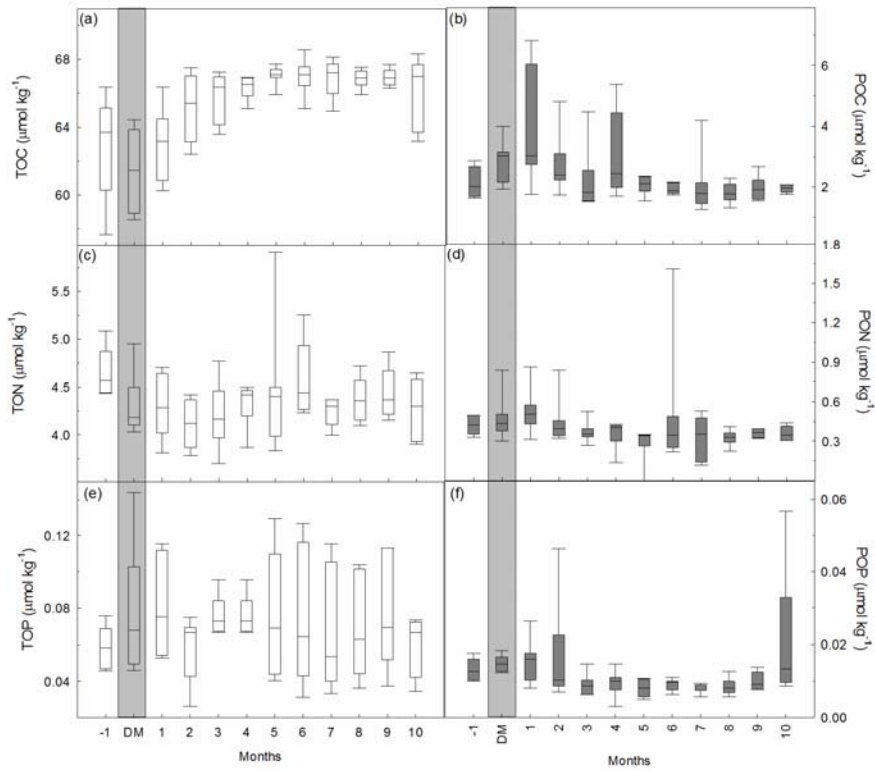
695

696

697

698 **Fig. 4**

Comment [MWL5]: New layout for figures 4-8 to improve clarity of the figure.



699

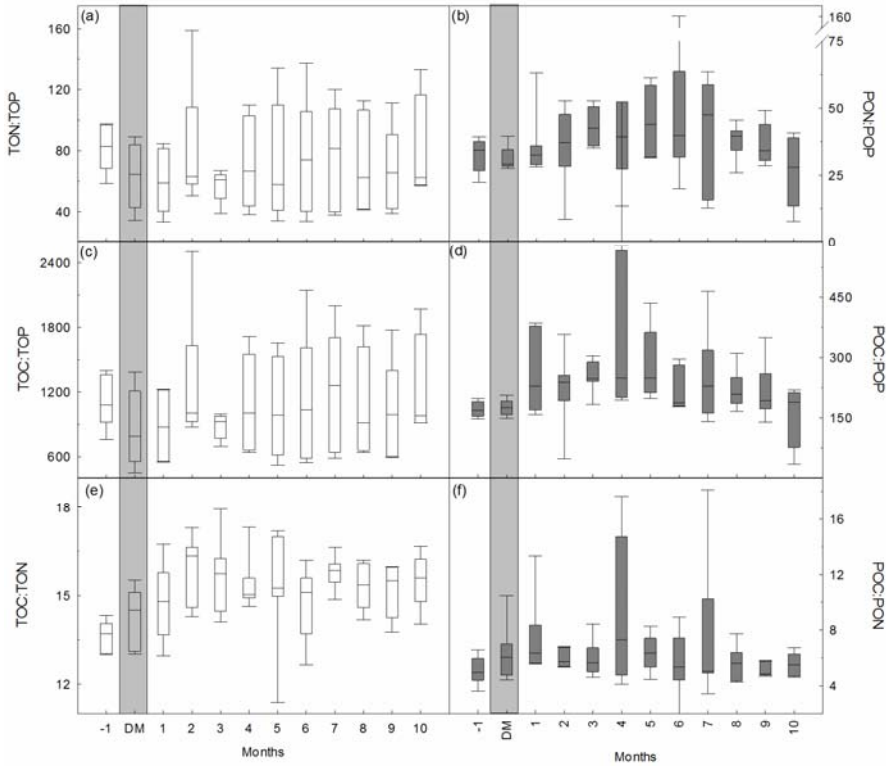
700

701

702

703

704 **Fig. 5**



705

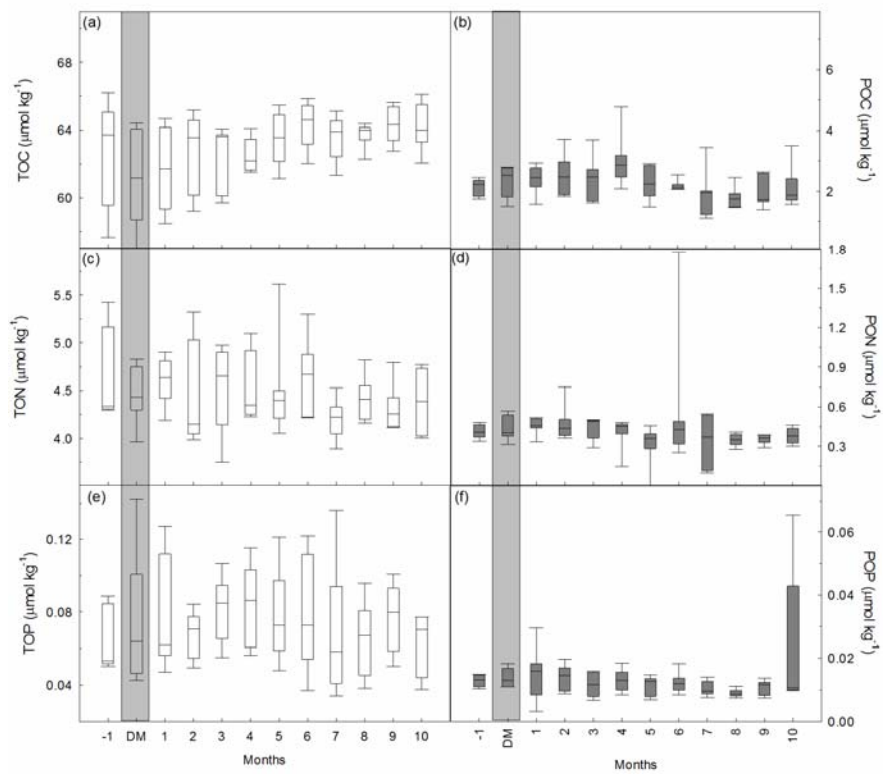
706

707

708

709

710 **Fig. 6**



711

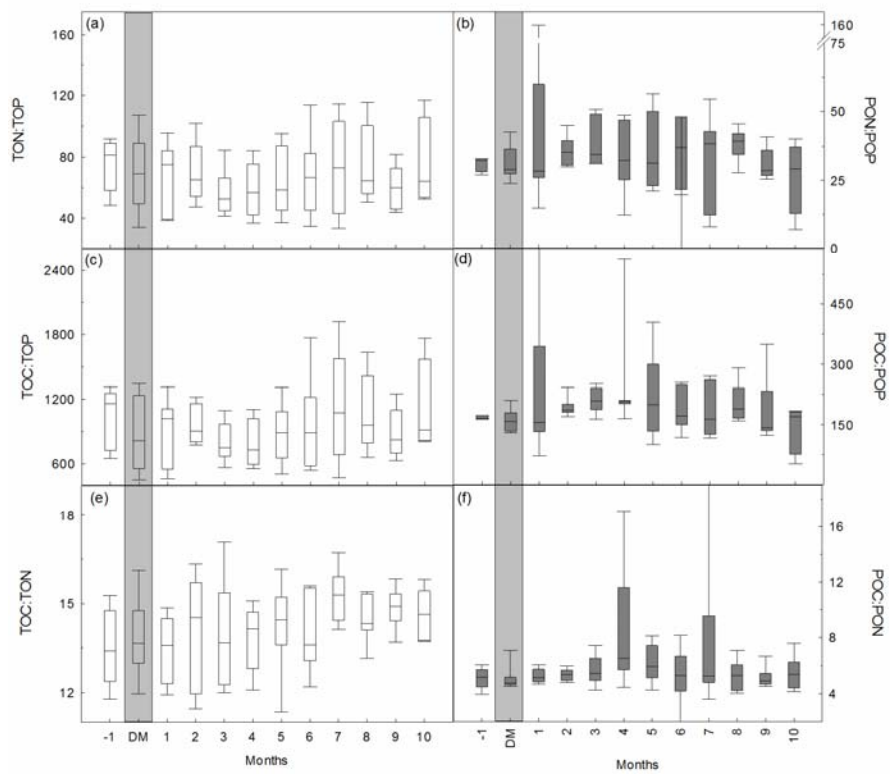
712

713

714

715

716 **Fig. 7**



717

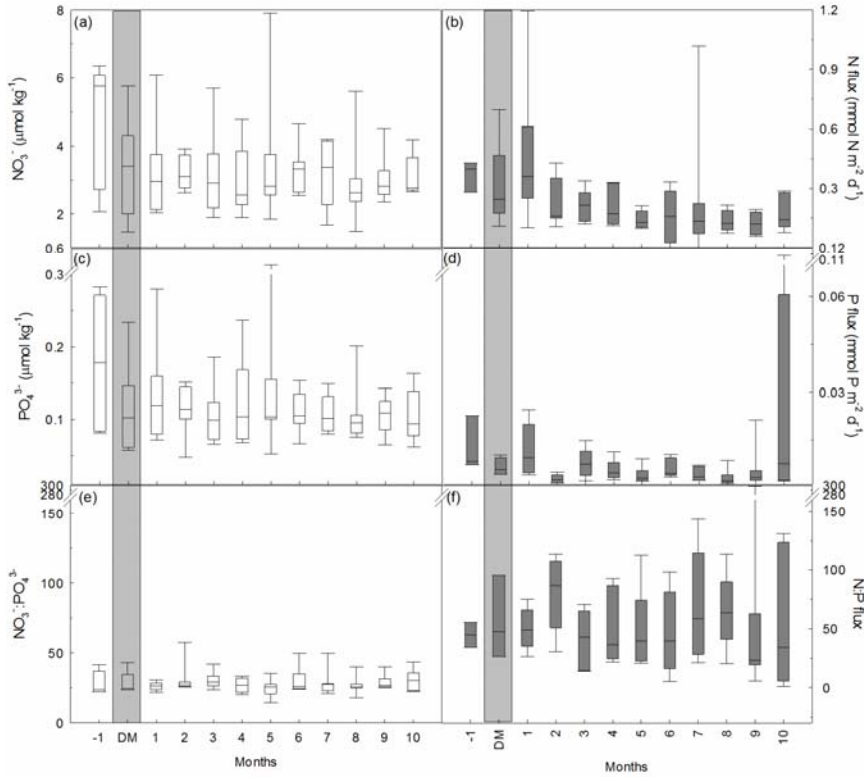
718

719

720

721

722 **Fig. 8**

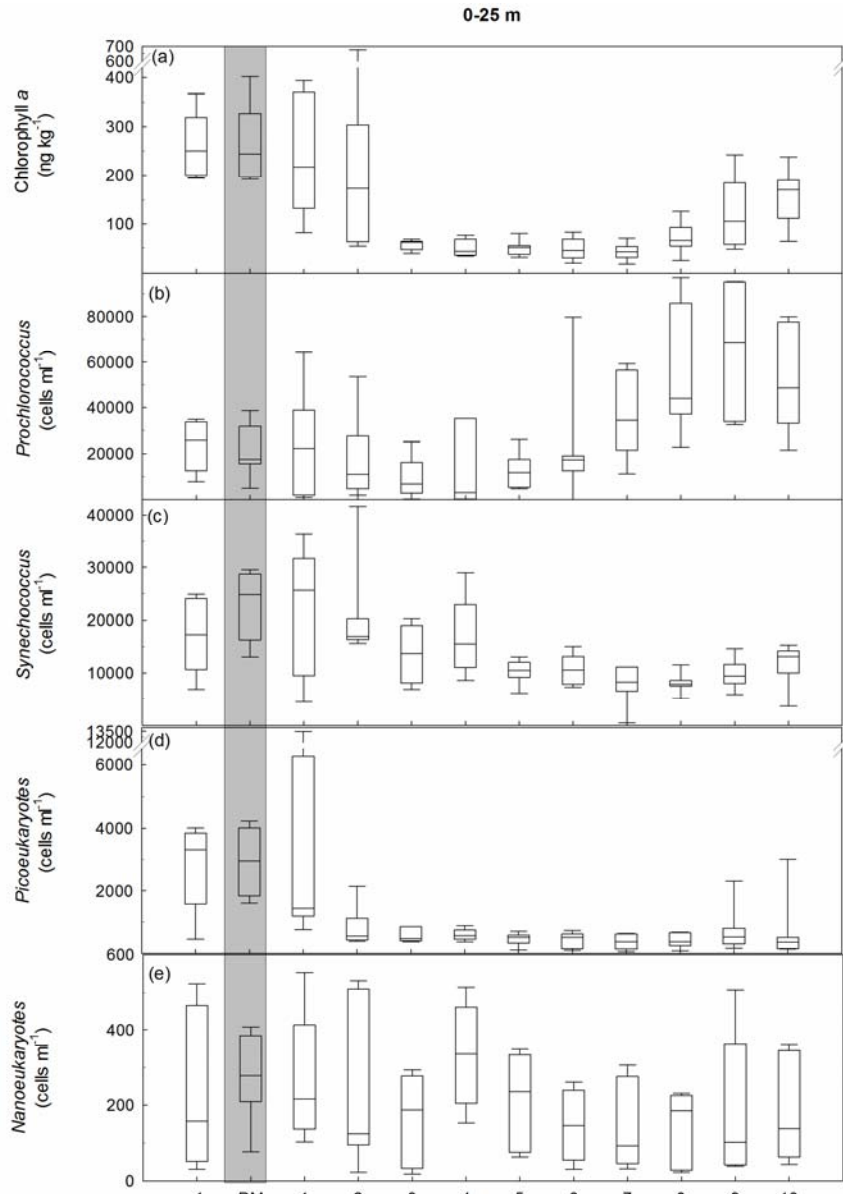


723

724

725

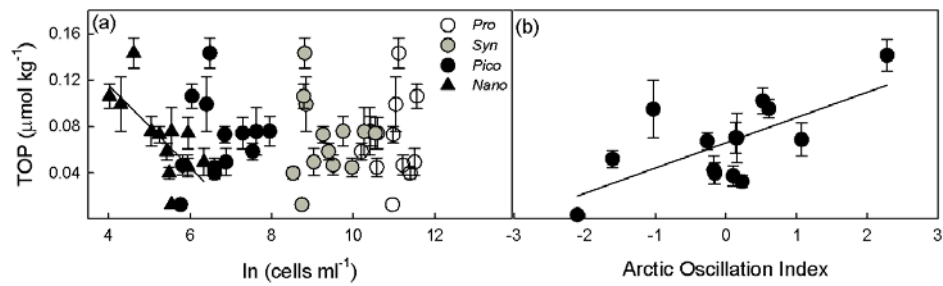
726



728

729

730 **Fig. 10**



731

732

733